

Dominant mutations in the tyrosyl-tRNA synthetase gene recapitulate in *Drosophila* features of human Charcot–Marie–Tooth neuropathy

Erik Storkebaum^{a,b,1}, Ricardo Leitão-Gonçalves^{a,b,c,d,1}, Tanja Godenschwege^e, Leslie Nangle^{f,9}, Monica Mejia^e, Inge Bosmans^{a,b}, Tinne Ooms^{c,d}, An Jacobs^{c,d}, Patrick Van Dijck^{h,i}, Xiang-Lei Yang^f, Paul Schimmel^{f,2}, Koen Norga^{a,j}, Vincent Timmerman^{c,d}, Patrick Callaerts^{a,b,1,3}, and Albena Jordanova^{c,d,1,4}

^aLaboratory of Developmental Genetics, ^bCenter for Human Genetics, ^cDepartment of Molecular Microbiology, ^dLaboratory of Molecular Cell Biology, Flanders Institute for Biotechnology (VIB), and ^eDepartment of Woman and Child, Children's Hospital, University of Leuven, BE-3000 Leuven, Belgium; ^fPeripheral Neuropathy Group, Department of Molecular Genetics, Flanders Institute for Biotechnology (VIB), and ^gNeurogenetics Laboratory, Institute Born-Bunge, University of Antwerp, BE-2610 Antwerp, Belgium; ^hDepartment of Biological Sciences, Florida Atlantic University, Boca Raton, FL 33431; ⁱThe Scripps Research Institute, La Jolla, CA 92037; and ^jTyr Pharma, San Diego, CA 92121

Contributed by Paul Schimmel, May 15, 2009 (sent for review January 31, 2009)

Dominant-intermediate Charcot–Marie–Tooth neuropathy (DI-CMT) is characterized by axonal degeneration and demyelination of peripheral motor and sensory neurons. Three dominant mutations in the *YARS* gene, encoding tyrosyl-tRNA synthetase (TyrRS), have so far been associated with DI-CMT type C. The molecular mechanisms through which mutations in *YARS* lead to peripheral neuropathy are currently unknown, and animal models for DI-CMT are not yet available. Here, we report the generation of a *Drosophila* model of DI-CMT: expression of the 3 mutant—but not wild type—TyrRS in *Drosophila* recapitulates several hallmarks of the human disease, including a progressive deficit in motor performance, electrophysiological evidence of neuronal dysfunction and morphological signs of axonal degeneration. Not only ubiquitous, but also neuron-specific expression of mutant TyrRS, induces these phenotypes, indicating that the mutant enzyme has cell-autonomous effects in neurons. Furthermore, biochemical and genetic complementation experiments revealed that loss of enzymatic activity is not a common feature of DI-CMT-associated mutations. Thus, the DI-CMT phenotype is not due to haploinsufficiency of aminoacylation activity, but most likely to a gain-of-function alteration of the mutant TyrRS or interference with an unknown function of the WT protein. Our results also suggest that the molecular pathways leading to mutant TyrRS-associated neurodegeneration are conserved from flies to humans.

aminoacylation | neurodegeneration | *YARS* | disease model | cell-autonomous

Charcot–Marie–Tooth disease (CMT)—also known as hereditary motor and sensory neuropathy (HMSN)—is the most common human inherited neuromuscular disorder, characterized by length-dependent axonal degeneration and demyelination of peripheral nerves (1). The main symptoms are progressive motor impairment, distal muscle wasting and weakness, sensory loss, reduced tendon reflexes, and foot deformities (2). Based on electrophysiological and histopathological criteria, CMT is divided into 2 major clinical entities: demyelinating forms of CMT (CMT1), in which nerve conduction velocities (NCVs) are severely reduced, and axonal forms (CMT2), in which NCVs are normal or slightly reduced. More recently, a third class has been added, dominant intermediate CMT (DI-CMT), which is characterized by slowly progressive neuropathy, intermediate NCVs and histological evidence of both axonal and demyelinating features (3).

We have reported that DI-CMT type C (DI-CMTC) is caused by dominantly inherited mutations in the gene *YARS*, encoding tyrosyl-tRNA synthetase (TyrRS) (4). TyrRS is an essential enzyme for protein biosynthesis and is expressed ubiquitously. It catalyzes the aminoacylation of tRNA^{Tyr} with tyrosine by a 2-step mechanism: tyrosine is first activated by ATP to form tyrosyl-adenylate and is then transferred to tRNA^{Tyr} (5). The functional enzyme is a

homodimer, and in each monomer 3 functional domains can be distinguished: an N-terminal catalytic domain, a central anticodon recognition domain, and a C-terminal EMAP II-like (endothelial monocyte-activating polypeptide II) domain (6). So far, 3 DI-CMTC-associated mutations have been identified, all located in the catalytic domain of the protein: 2 missense mutations (G41R and E196K) and one 12-bp in-frame deletion that results in the deletion of 4 amino acids in the TyrRS protein (153–156delVKQV). Interestingly, dominant mutations in the gene *GARS*, which encodes glycyl-tRNA synthetase (GlyRS), cause Charcot–Marie–Tooth disease type 2D (CMT2D) and distal SMA type V in humans and neuropathy phenotype in mice (7, 8). Because many of the disease-causing mutations in GlyRS do not affect the activity for aminoacylation or protein stability (9), and because *GARS* haploinsufficiency in the mouse does not lead to neuropathy (8), current speculation is that the neurodegenerative phenotype is caused by a gain of pathogenic function of mutant GlyRS, separable from aminoacylation. Indeed, expanded functions of tRNA synthetases in cell signaling pathways are now well known (10).

The present work was motivated by 2 considerations. First, pursuant to understanding the mechanistic link of a specific tRNA synthetase like TyrRS to CMT, we looked back through evolution. At the same time, we wanted to develop a simple experimental model for DI-CMTC. For these objectives, we set out to see whether we could establish a model for DI-CMTC in *Drosophila melanogaster* and whether the disease-causing mutant alleles identified in humans could also cause similar symptoms in a dominant way in flies. It is currently not established whether the disease is due to gain or loss of function, but the fact that all DI-CMTC-associated mutations are located in the catalytic domain raises the possibility that loss of aminoacylation activity could cause the disease through

Author contributions: E.S., R.L.-G., V.T., P.C., and A. Jordanova designed research; E.S., R.L.-G., T.G., L.N., M.M., I.B., T.O., A. Jacobs, and A. Jordanova performed research; T.G., P.V.D., X.-L.Y., and K.N. contributed new reagents/analytic tools; E.S., R.L.-G., T.G., and A. Jordanova analyzed data; and E.S., R.L.-G., P.S., V.T., P.C., and A. Jordanova wrote the paper.

The authors declare no conflict of interest.

Freely available online through the PNAS open access option.

¹E.S., R.L.-G., P.C., and A. Jordanova contributed equally to this work.

²To whom correspondence may be addressed. E-mail: schimmel@scripps.edu.

³To whom correspondence may be addressed at: Laboratory of Developmental Genetics, Flanders Institute for Biotechnology (VIB)-PRJ8 and Center for Human Genetics, University of Leuven, Herestraat 49, bus 602, B-3000 Leuven, Belgium. E-mail: patrick.callaerts@med.kuleuven.be.

⁴To whom correspondence may be addressed at: Department of Molecular Genetics, Flanders Institute for Biotechnology (VIB), University of Antwerp, Universiteitsplein 1, B-2610 Antwerpen, Belgium. E-mail: albena.jordanova@molgen.vib-ua.be.

This article contains supporting information online at www.pnas.org/cgi/content/full/0905339106/DCSupplemental.

haploinsufficiency. To address this issue, we performed biochemical and genetic complementation experiments to evaluate the effect of DI-CMTC-associated mutations in TyrRS on its aminoacylation activity. Furthermore, expression of mutant TyrRS in *Drosophila* induced neuronal phenotypes. This is in contrast to previous attempts by Chihara et al. (11), who could not identify dominant phenotypes by expression of 2 mutant forms of GlyRS in *Drosophila*. Thus, we have been able to generate a fly model for CMT, and it can be used to gain insights into the molecular pathogenesis of DI-CMTC. Our results show that the connection of TyrRS to neurodegeneration is deeply rooted in evolution and that this connection does not result from haploinsufficiency of the canonical aminoacylation function.

Results

Loss of Enzymatic Activity Is Not Common to DI-CMTC-Associated YARS Mutations. As in humans, the *Drosophila* genome contains a single gene encoding cytoplasmic tyrosyl-tRNA synthetase (*Aats-tyr*, for reasons of clarity hereafter referred to as *dYARS*). The *Drosophila* TyrRS protein (dTyrRS) is 68% identical and 80% similar to its human homolog (TyrRS), and all DI-CMTC mutated amino acid residues are strictly conserved between human and flies (Fig. S1). We therefore hypothesized that expression of human or *Drosophila* YARS mutants may induce similar molecular defects. To mimic the dominant inheritance pattern of DI-CMTC and to allow spatial control of transgene expression, we used the UAS-GAL4 system (12) to express WT or mutant YARS in flies. To ascertain that the phenotypes induced by expression of mutant YARS in *Drosophila* are not due to interspecies differences, we also generated *dYARS* transgenic flies, either WT or containing the DI-CMTC associated mutations. Lines with comparable expression levels were selected for further characterization (Fig. S2).

It is well known that tyrosyl-tRNA synthetases display species-specific tRNA^{Tyr} recognition, and therefore a synthetase from 1 species does not necessarily aminoacylate tRNA^{Tyr} from another species (13). We previously demonstrated that human TyrRS can aminoacylate yeast tRNA^{Tyr} (4). To investigate whether human TyrRS can also charge *Drosophila* tRNA^{Tyr} we performed an in vivo complementation assay. Expression of *dYARS-RNAi* in sensory organ precursor (SOP) cells leads to bristle phenotypes (Fig. 1A and B) that can be fully rescued by coexpression of *YARS.WT* (Fig. 1C and Fig. S3A), demonstrating that TyrRS and dTyrRS are functional homologs. The *dYARS-RNAi* induced bristle phenotypes can also be fully rescued with the mutant *YARS.E196K*, but not with the other 2 mutants (*YARS.G41R* and *YARS.153-156delVKQV*) (Fig. 1D–F and Fig. S3B–D). Because the link between enzymatic activity of TyrRS and peripheral nerve degeneration is a key question in DI-CMTC, we investigated possible differential effects of the 3 mutations on aminoacylation in additional experiments. In vivo genetic complementation in *S. cerevisiae* confirmed our findings in *Drosophila* (Fig. 1G). We previously demonstrated that both missense mutations (G41R and E196K) affect the first step of the aminoacylation reaction catalyzed by TyrRS, with G41R causing more severe reduction of the rate of tyrosine-dependent ATP-PPi exchange than E196K (4). However, because the second step is rate-limiting (5), and to confirm that our in vivo assays reflect enzymatic activity, we monitored the overall aminoacylation activity of mutant TyrRS proteins in an in vitro aminoacylation assay that measures directly the production of Tyr-tRNA^{Tyr} (14). In this assay, the G41R mutant showed almost complete loss of enzymatic activity, and the 153–156delVKQV mutant displayed significantly decreased activity. In contrast, the E196K mutant protein was fully active for aminoacylation (Fig. 1H). Thus, our in vivo and in vitro data demonstrate that loss of enzymatic activity is not common to DI-CMTC-associated TyrRS mutants.

Ubiquitous Expression of Mutant YARS Induces Impaired Motor Performance. Strong ubiquitous expression of mutant, but not WT, YARS, or *dYARS* induced full developmental lethality that could be reverted partially by reducing transgene expression levels (SI Text, Table S1, and Table S2). This indicates that mutant TyrRS induced developmental lethality is transgene dosage dependent, allowing analysis of adult-onset phenotypes. To determine whether mutant YARS-expressing flies exhibit motor performance defects, we investigated their behavior in a negative geotaxis climbing assay (15). *YARS.E196K* flies displayed severely impaired motor performance, because the average time needed to climb a vertical wall was increased by 65% compared with genetic controls (Fig. 2A and Movie S1). Flies expressing comparable levels of *YARS.G41R* or *YARS.153-156delVKQV* showed normal motor behavior, but higher level expression (2 copies of transgene) also induced severe motor impairment (Fig. 2A). In contrast, even high levels of *YARS.WT* did not impair motor performance, because the slight motor defect observed in actin5C-GAL4^{strong} > 2x *YARS.WT* flies (Fig. 2A) could be attributed to the presence of the actin5C-GAL4^{strong} driver (SI Text). Importantly, hemizygous *dYARS* flies displayed normal climbing behavior, indicating that reduction of *dYARS* gene dosage by 50% does not result in motor performance defects (SI Text). We further tested motor performance by jump and flight analysis (16). Aged *YARS.E196K* expressing flies displayed impairment in both jump and flight ability, because 92% of the flies failed to fly and 30% failed to jump (Table S3). Aged *YARS.G41R* and *YARS.153-156delVKQV* flies also displayed flight defects, because respectively 45% and 12% failed to fly. In contrast, aged *YARS.WT* flies were always able to jump and fly. Furthermore, analysis of jump and flight ability of mutant YARS flies at different ages revealed that these motor performance deficits are progressive (Fig. 2B and C), similar to the progressive motor impairment of DI-CMTC patients.

Neuron-Specific Expression of Mutant YARS Induces Impaired Motor Performance. We further tested whether neuron-specific expression of YARS transgenes could also induce motor performance defects, using the panneuronal elav-GAL4 and nsyb-GAL4 (17) drivers. Nsyb-GAL4 driven expression of moderate levels of *YARS.E196K* impaired motor performance by 74% (Fig. 2D), and expression of high levels of *YARS.E196K* (2 copies of transgene) resulted in the inability of flies to reach the top of the vial (Movie S2). Nsyb-GAL4 driven expression of high levels of *YARS.G41R* and *YARS.153-156delVKQV* also significantly impaired motor performance, in contrast to *YARS.WT* (Fig. 2D). Elav-GAL4 driven YARS expression induced motor performance defects only in *E196K* expressing flies (Fig. S4A). This difference between nsyb-GAL4 and elav-GAL4 induced phenotypes can be explained by the fact that nsyb-GAL4 drives stronger transgene expression (Fig. S4B). Nsyb-GAL4 driven expression of the 3 mutant—but not WT—*dYARS* alleles also induced defects in climbing behavior (Fig. 2E), indicating that TyrRS and dTyrRS induce similar phenotypes. To determine whether the motor performance deficit induced by panneuronal expression of mutant YARS is due to massive degeneration of neuronal cell bodies (which is characterized by vacuolization of the fly brain), or rather a consequence of more subtle neuronal dysfunction and/or axonal degeneration (as is the case in CMT patients), histological analysis was performed. This analysis revealed that nsyb-GAL4 > mutant YARS expression is not accompanied by overt neurodegeneration in the brain or ventral nerve cord, because no vacuolization could be found (Fig. S4C and D). Specific expression of high levels of *YARS.E196K* in muscle (MHC-GAL4) did not impair motor performance (SI Text). Thus, motor dysfunction in flies expressing mutant YARS ubiquitously is at least in part because of cell-autonomous effects in neurons.

Expression of Mutant YARS in the Giant Fiber System Induces Electrophysiological and Morphological Neuronal Defects. To characterize neuronal dysfunction further, we focused on the giant fiber

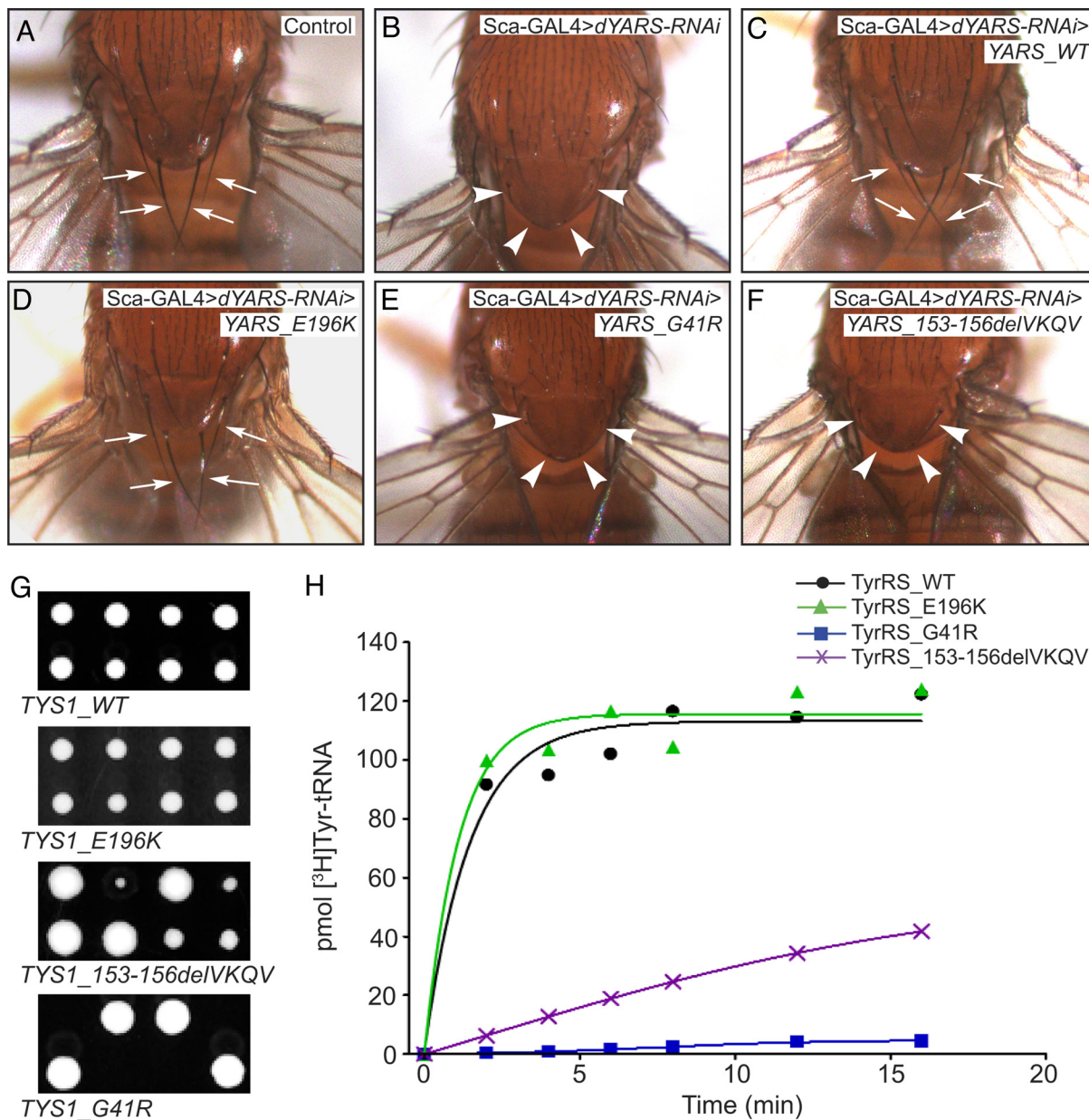


Fig. 1. Loss of enzymatic activity is not common to DI-CMTC associated TyrRS mutations. (A–C) TyrRS and dTyrRS are functional homologs. Scabrous-GAL4-driven expression of *dYARS-RNAi* induced bristle phenotypes: scutellar bristles (arrows in A) were often shorter or missing, with the dorsal scutellar bristles displaying more severe defects than the anterior scutellar bristles (arrowheads in B). This was never the case in genetic controls (A). *YARS.WT* coexpression (C) resulted in full rescue of scabrous-GAL4 > *dYARS-RNAi* induced bristle phenotypes. (D–F) *dYARS-RNAi* induced bristle phenotypes could also be fully rescued by coexpression of *YARS.E196K* (D), but not by *YARS.G41R* (E) and *YARS.153-156delVKQV* (F). (G) Genetic complementation experiments in *S. cerevisiae*. Single copy plasmids encoding WT or mutant *TYS1* (the *S. cerevisiae* *YARS* ortholog) under the regulation of its native promoter and terminator were transformed into a hemizygous *TYS1*-deletion strain. Transformants were sporulated and resulting tetrads were dissected to obtain haploid spores. Viability of 50% of the spores depends on the aminoacylation activity of the transgene. Segregant colonies expressing *TYS1.WT* or *TYS1.E196K* had normal colony size, consistent with normal aminoacylation activity. *TYS1.153-156delVKQV* colonies were viable but displayed reduced colony size and *TYS1.G41R* colonies were nonviable, indicative for severe reduction of aminoacylation activity. (H) Enzymatic activity of recombinant full-length WT and mutant TyrRS proteins determined in an in vitro aminoacylation assay (14).

(GF) system, a neuronal network that mediates an escape response consisting of a jump and subsequent flight (18). Importantly, it contains one of the longest axons in *Drosophila*, making it particularly relevant to model CMT. We expressed *YARS* in the GF system and used electrophysiology to record the response latency and the ability to follow stimuli one-to-one at high frequencies, as measures of synaptic strength and synaptic reliability, respectively. Simultaneous presynaptic and postsynaptic expression (A307-GAL4 driver) of mutant, but not WT, *YARS* in the GF and its motor neuron targets resulted in

neuronal dysfunction (Fig. 2F). Some flies had normal response latencies but had defects in following high frequency stimulation whereas the more severely affected flies displayed increased response latencies as well. In a few cases, no response of the GF-tergotrochanteral muscle (TTM) pathway was observed upon brain stimulation while the GF-dorsal longitudinal muscles pathway was still present. Thoracic stimulation revealed that the defect was in the giant synaptic terminal between the GF and the tergotrochanteral motoneuron (TTMn). All 3 *YARS* mutations induced these defects. The severity and frequency of the mutant

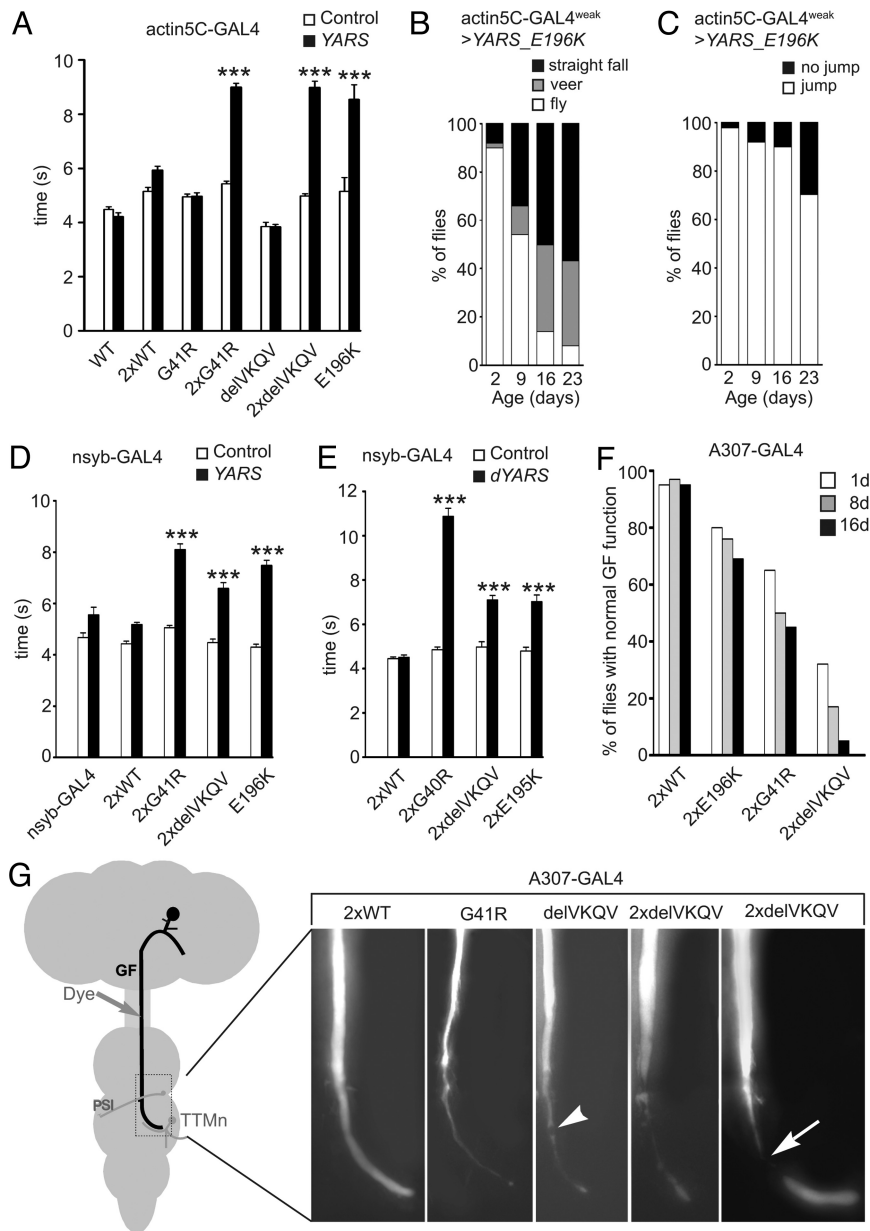


Fig. 2. Expression of mutant YARS in *Drosophila* induces impaired motor performance, electrophysiological evidence of neuronal dysfunction, and defects in axon terminal morphology. (A) Impaired performance of mutant YARS flies in a negative geotaxis climbing assay. The average time needed to climb a vertical wall to a height of 82 mm is displayed. Actin5C-GAL4^{weak} was used to drive 1 copy of transgene; actin5C-GAL4^{strong} was used to drive 2 copies of transgene. Control flies carry transgenes without driver. (B and C) Flight (B) and jump (C) ability of actin5C-GAL4^{weak} >YARS_E196K flies progressively declines with age. In a flight assay (16), the percentage of flies that fell in a straight line, fell by veering or flew was determined at the indicated ages (B). The same flies were tested for jumping ability (16) (C). All genetic control flies were able to fly and jump at all ages tested (see Table S3). (D) Specific expression of mutant YARS in neurons induced impaired motor performance in a negative geotaxis assay. Nsyb-GAL4 was used to drive 2 copies of YARS transgenes, flies lacking the driver were used as controls. (E) Negative geotaxis assay on nsyb-GAL4 > 2x dYARS flies revealed impaired motor performance in flies expressing mutant—but not WT—dYARS panneuronally. (F) Electrophysiological defects in the giant fiber system of mutant YARS expressing flies. The percentages of flies without electrophysiological synaptic defects are shown for each age group. More than 20 female flies carrying A307-GAL4 and 2 copies of YARS transgene were tested for each age group. A functional defect is defined as a response latency > 1 ms and/or the inability to follow 100-Hz stimuli one-to-one. All comparisons of mutant YARS versus YARS_WT are statistically significant, except for the 1-day time point where 2x E196K and 2x G41R are not significantly different from WT. (G) To determine the correlation between GF function and morphology, dye-filling experiments were performed of electrophysiologically tested flies, which revealed the morphology of the giant fiber. In flies with no physiological phenotype or with defects only in following stimuli at 100 Hz, no gross anatomical defects were seen. In 100% of flies with increased response latency or no TTM response upon brain stimulation, the giant synaptic terminal was abnormally thin with occasional vesicles (arrowhead) or exhibited constrictions (arrow). A307-GAL4 was used to drive expression of the indicated transgenes. ***, $P < 0.001$; indicates significant differences versus genetic controls, as determined by one-way ANOVA with Bonferroni's Multiple Comparison Test.

phenotypes increased with age (Fig. 2F), indicating that the phenotypes are progressive and similar to what is seen in DI-CMTC patients and in our previous experiments (Fig. 2B and C). Selective presynaptic expression of YARS_153-

156delVKQV in the GF (C17-GAL4 driver) induced defects in 38% of 8-day-old flies ($n = 16$), whereas selective expression in the postsynaptic TTMn (Shak-B-GAL4) had no effect ($n = 16$), indicating that the functional defects are purely presynaptic. Dye

injections in GFs further revealed morphological deficits of the GF terminal, which was abnormally thin with occasional vesicles or constrictions (Fig. 2G). Furthermore, analysis at different ages indicated that the axon terminal slowly degenerates over time. Thus, expression of mutant, but not WT, *YARS* in a subset of neurons induced electrophysiological and morphological defects.

Discussion

We report the generation of a *Drosophila* model for CMT and an animal model for DI-CMTC. *D. melanogaster* was used as a genetic model organism for DI-CMTC, because of the multitude of genetic tools available (19), the significant conservation of fundamental biological pathways between humans and flies (20), and its proven usefulness to model human neurodegenerative disorders (21, 22). Our initial choice to express human TyrRS in *Drosophila* was based on the unusually high evolutionary conservation between *Drosophila* and human proteins. This choice can now further be justified by our findings that dTyrRS and TyrRS are functional homologs, and that expression of *dYARS* containing DI-CMTC-associated mutations induces developmental lethality and motor performance deficits in a similar way as mutant *YARS*. Therefore, expression of mutant *YARS* can be expected to induce similar molecular derailments in *Drosophila* and humans.

In contrast to WT *YARS*, expression of the 3 DI-CMTC associated *YARS* mutants induced phenotypes that successfully recapitulate some of the hallmarks of the human disease, including progressive motor performance deficits, electrophysiological evidence of neuronal dysfunction, and terminal axonal degeneration. Furthermore, tissue-specific mutant *YARS* expression also induced eye, wing, and bristle phenotypes (Fig. S5), which can be used in future genetic screens for putative disease modifying genes, an experimental approach for which *Drosophila* is ideally suited (23). Our *Drosophila* DI-CMTC model will also be useful to screen drug libraries to identify potential therapeutic compounds, as reported before for *Drosophila* models of other neurodegenerative disorders (24, 25). Moreover, an important finding is that not only ubiquitous, but also neuron-specific expression of mutant *YARS* induces impaired motor performance and electrophysiological and morphological neuronal defects. Indeed, DI-CMTC patients display both demyelination and axonal degeneration, and it is not known whether either axons or Schwann cells are the primary target of the disease, or whether the initial pathological events occur in both cell types simultaneously (3). Our data demonstrate a neuronal contribution to DI-CMTC, suggesting that the axonal degeneration observed in patients is not just secondary to demyelination. Our observation that neuron-specific expression of mutant *YARS* is sufficient to induce neuronal defects does not exclude the possibility that in DI-CMTC patients other cell types (such as Schwann cells) contribute to axonal pathology in a non-cell-autonomous way. Further research in mammals is needed to determine if, and to which extent, Schwann cell pathology contributes to DI-CMTC.

We further studied aminoacylation activity of the 3 DI-CMTC-associated TyrRS mutants, both in vitro and in vivo in *S. cerevisiae* and *D. melanogaster*. These studies consistently demonstrated that the E196K mutant has normal enzymatic activity, whereas enzymatic activity was severely reduced for the 153–156delVKQV protein and almost completely lost for the G41R mutant. Furthermore, hemizygous *dYARS* flies display normal motor performance, despite 50% reduction of *dYARS* gene dosage. Together, these data indicate that loss of aminoacylation activity is neither necessary nor sufficient to cause peripheral neuropathy. A similar conclusion has been drawn for CMT2D-associated mutations in GlyRS. Indeed, approximately half of the GlyRS mutations have no effect on aminoacylation activity, whereas the other half displays severe reduction or loss of aminoacylation activity (9, 26). Furthermore, in a CMT2D mouse model, a GlyRS P278KY mutation—which does not correspond to a human CMT2D mutation—gives rise to peripheral neuropathy, despite normal expression and normal

aminoacylation activity of GlyRS (8). Finally, an A734E mutation in alanyl-tRNA synthetase that causes cerebellar ataxia in mice does not impair aminoacylation activity, but results in a mild editing defect so that the enzyme cannot deacylate Ser-tRNA^{Ala} (27). In contrast, tyrosyl-tRNA synthetase has no known editing activity. All of these findings consistently reveal that the role of aminoacyl-tRNA synthetases in neurodegeneration is complex and not necessarily directly related to aminoacylation. Rather, CMT-associated mutations in aminoacyl-tRNA synthetases might disrupt non-canonical functions of these proteins, or result in a dominant “gain of toxic function.”

Commonly, expanded functions of tRNA synthetases, including those for tyrosyl-tRNA synthetase, are activated by alternative splicing, proteolysis, or post-translational modification, and act on extracellular or intracellular targets (28–30). An expanded function of human TyrRS in endothelial cells was mutationally separated from that for aminoacylation, that is, mutations were isolated that disrupted cell signaling, but not aminoacylation, and vice versa (31). This result is reminiscent of what is reported here, namely, neuronal expression of *YARS.E196K* induces strong motor performance deficits despite normal TyrRS aminoacylation activity. Interestingly, because we have been able to recapitulate in the fly pathological features of the human disease, we infer that the molecular pathways leading to mutant TyrRS associated neurodegeneration were established long before the appearance of mammals. In this context, the fly model we generated can be used to gain mechanistic insight into the molecular pathogenesis of DI-CMTC, into the role of tyrosyl-tRNA synthetase in neuronal cell homeostasis and for the development of new therapeutic strategies.

Materials and Methods

DNA Construction and Generation of Transgenic Flies. Full-length *YARS* cDNA was obtained from the RZPD (German Resource Center for Genome Research) collection, clone IMAGp998G1110070Q. Full-length *dYARS* cDNA (clone LD21116) was obtained from the BDGP *Drosophila* Gold Collection. Mutations in *YARS* and *dYARS* cDNA were created with the Quick Change mutagenesis kit (Stratagene). *YARS* or *dYARS* cDNA with or without the appropriate mutations were subcloned into the pUAST transformation vector. All constructs were sequence verified and transgenic flies were generated using standard procedures. For each construct, multiple transgenic lines were established and expression levels were determined by western blot or quantitative real time PCR. See *SI Text* for details on western blot and qRT-PCR analysis.

***Drosophila* Genetics.** The *nsyb-GAL4* driver line (17) was kindly provided by M. Leyssen and B. Dickson. Other GAL4 driver lines and *dYARS* deficiency lines described in this paper were obtained from the Bloomington *Drosophila* Stock Center. *dYARS-RNAi* lines were obtained from the National Institute of Genetics (NIG, Japan). For the determination of adult offspring frequencies, the number of adult flies eclosing for each genotype was counted. For quantification of scabrous-GAL4 induced bristle phenotypes, anterior and posterior scutellar bristles were examined and the number of normal, small or missing bristles was determined and the relative percentages were calculated.

Protein Production, Purification, and Aminoacylation Analysis. Recombinant human full-length WT and mutant TyrRS proteins with a C-terminal 6 histidine tag were produced and purified, and protein concentration was determined using the Bradford assay (Bio-Rad). The aminoacylation assay was performed as described in ref. 14. See *SI Text* for experimental details.

Yeast Strain, Growth, and Tetrad Analysis. WT or G45R, E200K and 157–160delVKQV *TYR1* (corresponding to G41R, E196K, and 153–156delVKQV mutations in *YARS*, respectively) was cloned into a single-copy plasmid (YCplac111) under the regulation of its native promoter and terminator. The *S. cerevisiae* hemizygous *TYR1*-deletion strain Y24815 (*MA*Talalpha *his3/his3 leu2/leu2 ura3/ura3 met15/MET15 LYS2/lys2 TYR1/tyr1::KAN^R*) was obtained from the Euroscarf collection (Invitrogen). The yeast strain was transformed with plasmid DNA using the lithium acetate method and transformants were cultured on selective media. Tetrad analysis was performed as described in ref. 4.

***Drosophila* Behavioral Assays.** To assay adult motor performance, negative geotaxis, jump, and flight ability were analyzed. Walking speed in negative

geotaxis was determined as described in ref. 15, with some slight modifications (Movie S1). Briefly, 10 female flies with shortened wings were shaken down to the bottom of a cylindrical fly container (49-mm diameter) that was covered with a black cap. The experiment was carried out on a black surface under red light. Time needed for the first fly from the start of the ascent at the vertical wall to a mark at a height of 82 mm was measured. For each group of 10 flies, the experiment was done 10 times and the average of these 10 walking speeds was calculated. For each genotype, 10 groups of 10 flies were tested. Jump and flight ability were analyzed as described in ref. 16. Fifty flies of each genotype were assayed.

Luciferase Assay. Luciferase was measured using the Promega Steady-Glo Luciferase Assay Kit, as described in ref. 32. See *SI Text* for experimental details.

Histology. For paraffin embedding, flies were fixed for 1 hour in 4% formaldehyde on ice. After washing in PBS, flies were dehydrated and transferred successively to a 1:1 mixture of ethanol:methylbenzoate, methylbenzoate, a 1:1 mixture of methylbenzoate:paraffin, and paraffin. After paraffin embedding, 7- μ m transverse sections through whole flies were made and stained with hematoxylin and eosin.

Giant Fiber Assays. Electrophysiology. Intracellular recordings from muscles of adult female flies were obtained following (33) with modification as described in ref. 34. In brief, the giant fibers were activated extracellularly in brain by 2 etched tungsten electrodes (one placed through each eye) using short pulses of 0.03 ms (Grass S44 stimulator, Grass Instruments). Thoracic stimulation was used to stimulate the motor neurons directly. A tungsten electrode placed in the abdominal cavity served as a ground. Glass electrodes filled with saline were inserted through the cuticle into the TTM and DLM muscle fibers. The recordings were amplified (Getting 5A amplifier, Getting Instruments) and the signals stored on a PC using pCLAMP software and a Digidata 1440 interface (Molecular Devices).

Each animal was given single stimulations 10 times to determine the average response latency and 10 trials of 10 pulses at 100 Hz to determine the ability of the synapse to follow stimuli at high frequencies.

Dye injections into the giant fiber. The dissected CNS was mounted dorsal side up on a slide coated with polylysine and the preparation was immersed in saline. A glass electrode (60–80 M Ω) containing 1% aqueous Lucifer yellow and backfilled with 3M LiCl was used to impale the GF in the connective. The dye was injected into the GF by the passage of hyperpolarizing current. Z-stack images were taken using an advanced SPOT camera and MetaVue software. Deconvolution was carried out on images using Autovisualize and AutoBlur software (Autoquant).

Statistics. We used SPSS 16.0 and GraphPad Prism 4 software for statistical calculations. χ^2 statistics were used to analyze offspring frequency and GF electrophysiology data. One-way ANOVA with Bonferroni's Multiple Comparison Test was used to analyze negative geotaxis and luciferase assay data. For all other data, unpaired *t* test was used for statistical analysis. All data are reported as the mean \pm SEM.

ACKNOWLEDGMENTS. We thank L. Vanden Broeck, S. Uthaman, M. Deprez, I. Pintens, W. Robyns, and A. Schellens for technical and editorial assistance; M. Leyssen and B. Dickson (Research Institute of Molecular Pathology, Vienna, Austria) for providing the *nsyb-GAL4* driver line; and M. Markstein (Harvard Medical School) for providing the *UAS::Luciferase* lines. This work is supported by University of Antwerp's Special Research Fund and Methusalem program, Katholieke Universiteit Leuven (OT/06/53/TBA), Research Foundation Flanders (FWO) Grants G024508N and G039706N, Interuniversity Attraction Poles program (P6/43) of the Belgian Federal Science Policy Office, Medical Foundation Queen Elisabeth, Association Belge contre les Maladies Neuromusculaires, American National Institute of Child Health and Human Development Grant R01HD050725, National Institutes of Health Grants GM15539 and GM2356, and National Foundation for Cancer Research. E.S., R.L.-G., and K.N. are supported by the Fund for Scientific Research (FWO-Flanders, Belgium).

- Suter U, Scherer SS (2003) Disease mechanisms in inherited neuropathies. *Nat Rev Neurosci* 4:714–726.
- Dyck PJ (1993) in *Peripheral Neuropathy* (Saunders Company, Philadelphia), pp 1094–1136.
- Nicholson G, Myers S (2006) Intermediate forms of Charcot-Marie-Tooth neuropathy: A review. *Neuromol Med* 8:123–130.
- Jordanova A, et al. (2006) Disrupted function and axonal distribution of mutant tyrosyl-tRNA synthetase in dominant intermediate Charcot-Marie-Tooth neuropathy. *Nat Genet* 38:197–202.
- Schimmel PR, Soll D (1979) Aminoacyl-tRNA synthetases: General features and recognition of transfer RNAs. *Annu Rev Biochem* 48:601–648.
- Kleeman TA, Wei D, Simpson KL, First EA (1997) Human tyrosyl-tRNA synthetase shares amino acid sequence homology with a putative cytokine. *J Biol Chem* 272:14420–14425.
- Antonellis A, et al. (2003) Glycyl tRNA synthetase mutations in Charcot-Marie-Tooth disease type 2D and distal spinal muscular atrophy type V. *Am J Hum Genet* 72:1293–1299.
- Seburn KL, Nangle LA, Cox GA, Schimmel P, Burgess RW (2006) An active dominant mutation of glycyl-tRNA synthetase causes neuropathy in a Charcot-Marie-Tooth 2D mouse model. *Neuron* 51:715–726.
- Nangle LA, Zhang W, Xie W, Yang XL, Schimmel P (2007) Charcot-Marie-Tooth disease-associated mutant tRNA synthetases linked to altered dimer interface and neurite distribution defect. *Proc Natl Acad Sci USA* 104:11239–11244.
- Park SG, Schimmel P, Kim S (2008) Aminoacyl tRNA synthetases and their connections to disease. *Proc Natl Acad Sci USA* 105:11043–11049.
- Chihara T, Luginbuhl D, Luo L (2007) Cytoplasmic and mitochondrial protein translation in axonal and dendritic terminal arborization. *Nat Neurosci* 10:828–837.
- Brand AH, Perrimon N (1993) Targeted gene expression as a means of altering cell fates and generating dominant phenotypes. *Development* 118:401–415.
- Bonnefond L, Giege R, Rudinger-Thirion J (2005) Evolution of the tRNA(Tyr)/TyrRS aminoacylation systems. *Biochimie* 87:873–883.
- Schreiber AA, Schimmel PR (1972) Transfer ribonucleic acid synthetase catalyzed deacylation of aminoacyl transfer ribonucleic acid in the absence of adenosine monophosphate and pyrophosphate. *Biochemistry* 11:1582–1589.
- Strauss R, Heisenberg M (1993) A higher control center of locomotor behavior in the *Drosophila* brain. *J Neurosci* 13:1852–1861.
- Pesah Y, et al. (2004) *Drosophila* parkin mutants have decreased mass and cell size and increased sensitivity to oxygen radical stress. *Development* 131:2183–2194.
- Pauli A, et al. (2008) Cell-type-specific TEV protease cleavage reveals cohesin functions in *Drosophila* neurons. *Dev Cell* 14:239–251.
- Allen MJ, Godenschwege TA, Tanouye MA, Phelan P (2006) Making an escape: Development and function of the *Drosophila* giant fibre system. *Semin Cell Dev Biol* 17:31–41.
- Venken KJ, Bellen HJ (2005) Emerging technologies for gene manipulation in *Drosophila melanogaster*. *Nat Rev Genet* 6:167–178.
- Rubin GM, et al. (2000) Comparative genomics of the eukaryotes. *Science* 287:2204–2215.
- Marsh JL, Thompson LM (2006) *Drosophila* in the study of neurodegenerative disease. *Neuron* 52:169–178.
- Bilen J, Bonini NM (2005) *Drosophila* as a model for human neurodegenerative disease. *Annu Rev Genet* 39:153–171.
- St Johnston D (2002) The art and design of genetic screens: *Drosophila melanogaster*. *Nat Rev Genet* 3:176–188.
- Chang S, et al. (2008) Identification of small molecules rescuing fragile X syndrome phenotypes in *Drosophila*. *Nat Chem Biol* 4:256–263.
- Steffan JS, et al. (2001) Histone deacetylase inhibitors arrest polyglutamine-dependent neurodegeneration in *Drosophila*. *Nature* 413:739–743.
- Xie W, Nangle LA, Zhang W, Schimmel P, Yang XL (2007) Long-range structural effects of a Charcot-Marie-Tooth disease-causing mutation in human glycyl-tRNA synthetase. *Proc Natl Acad Sci USA* 104:9976–9981.
- Lee JW, et al. (2006) Editing-defective tRNA synthetase causes protein misfolding and neurodegeneration. *Nature* 443:50–55.
- Greenberg Y, et al. (2008) The novel fragment of tyrosyl tRNA synthetase, mini-TyrRS, is secreted to induce an angiogenic response in endothelial cells. *FASEB J* 22:1597–1605.
- Kapoor M, et al. (2008) Evidence for annexin II-S100A10 complex and plasmin in mobilization of cytokine activity of human TrpRS. *J Biol Chem* 283:2070–2077.
- Ray PS, et al. (2009) A stress-responsive RNA switch regulates VEGFA expression. *Nature* 457:915–919.
- Kapoor M, Otero FJ, Slike BM, Ewalt KL, Yang X-L (2009) Mutational separation of aminoacylation and cytokine activities of human tyrosyl-tRNA synthetase. *Chem Biol* 16:531–539.
- Markstein M, Pitsouli C, Villalta C, Celniker SE, Perrimon N (2008) Exploiting position effects and the gypsy retrovirus insulator to engineer precisely expressed transgenes. *Nat Genet* 40:476–483.
- Tanouye MA, Wyman RJ (1980) Motor outputs of giant nerve fiber in *Drosophila*. *J Neurophysiol* 44:405–421.
- Godenschwege TA, Hu H, Shan-Crofts X, Goodman CS, Murphey RK (2002) Bidirectional signaling by Semaphorin 1a during central synapse formation in *Drosophila*. *Nat Neurosci* 5:1294–1301.